



## Iron(III) complexes of bis (benzimidazol-2-yl) methyl thiophene-2,5-dicarboxamide: Synthesis, spectral and oxidation of *o*-phenylenediamine

Nidhi Tyagi, Pavan Mathur\*

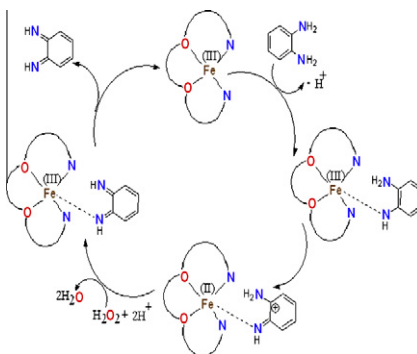
Department of Chemistry, University of Delhi, Delhi 110007, India

### HIGHLIGHTS

- ▶ Iron(III) complexes of a bisbenzimidazolyl diamide ligand.
- ▶ EPR, Mössbauer indicate axially distorted complexes.
- ▶ Complexes catalyze the oxidation of *o*-phenylenediamine.
- ▶ Effect of added anion on the rate of reaction.
- ▶ Implication of Fe(III) in inner sphere electron transfer.

### GRAPHICAL ABSTRACT

New iron(III) complexes have been utilized as catalysts for the oxidation of *o*-phenylenediamine to 2,3-diaminophenazine in the presence  $\text{H}_2\text{O}_2$ . The effect of added exogenous anion like acetate, azide and citrate, is found to inhibit the rate of reaction suggesting that one of the factors affecting the rate determining step is the loss of bound  $\text{Cl}^-$ ,  $\text{NO}_3^-$  at the iron(III) centre, creating a vacant site and the concomitant binding of exogenous anions or *o*-phenylenediamine.



### ARTICLE INFO

#### Article history:

Received 14 February 2012  
Received in revised form 12 June 2012  
Accepted 5 July 2012  
Available online 20 July 2012

#### Keywords:

Bis-benzimidazolyl thiophene diamide  
Iron(III)  
*o*-Phenylenediamine  
2,3-Diaminophenazine

### ABSTRACT

Iron(III) complexes of a potentially pentadentate ligand  $\text{N}^2, \text{N}^5$ -bis ((1H-benzo [d] imidazol-2-yl) methyl) thiophene-2,5-dicarboxamide are synthesized with an exogenous anion  $\text{X} = \text{Cl}^-, \text{NO}_3^-$ . Mössbauer and EPR spectroscopy indicates axially distorted complexes. These complexes were utilized for the oxidation of *o*-phenylenediamine to 2,3-diaminophenazine in presence of  $\text{H}_2\text{O}_2$ . The initial rate of reaction is dependent on the concentration of *o*-phenylenediamine as well as the iron(III) complex. Rates of reaction were found to be at least five times higher for the  $\text{Cl}^-$  bound complex. The effect of an added anion like acetate, azide and citrate is found to inhibit the rate of reaction. This suggests that one of the factors affecting the rate determining step is the binding of these anions on a vacant site at the iron(III) centre. The oxidation of *o*-phenylenediamine to 2,3-diaminophenazine is reminiscent of the functioning of horse radish peroxidase.

© 2012 Elsevier B.V. All rights reserved.

### Introduction

Peroxidases catalyze the reduction of hydrogen peroxide produced as an intermediate during the reduction of molecular oxy-

gen in the process of respiration [1]. Horse radish peroxidase (HRP) is an iron containing enzyme that belongs to the class of peroxidases. In its catalytic cycle horse radish peroxidase binds the peroxidyl group to the iron(III) center in the active site and reduces it to a water molecule, generating the oxo-ferryl form of HRP. This species is then capable of oxidizing organic substrates like phenols, amines and catechol amines [2]. HRP has been found

\* Corresponding author. Tel.: +91 11 27667725x1381; fax: +91 11 27666605.  
E-mail address: [pavanmat@yahoo.co.in](mailto:pavanmat@yahoo.co.in) (P. Mathur).

to be extremely effective catalyst for the oxidation of *o*-phenylenediamine to 2,3-diaminophenazine [2–5], while other iron containing enzymes that catalyze this oxidation are methemoglobin [6] hemoglobin [7] and cytochrome *c* [8].

Oxidation of *o*-phenylenediamine has been reported in the presence of Co(II) salts occurring via  $\mu$ -peroxodicobalt(III) and oxocobalt(IV) complex as intermediates [9] and cobaloxime(II) derivatives have been used for the oxidation of *o*-phenylenediamine by atmospheric oxygen at ambient temperature [10]. While tris-oxalato complexes of Co(III), Mn(III) and Cu(II) have also been reported for the oxidation of *o*-phenylenediamine to 2,3-diaminophenazine using resins support [11].

Potassium ferricyanide [12], iron tetrasulphophthalocyanine [13], and iron(III) tetra-(*N*-methyl-4-pyridyl)-porphyrin [2], are few of iron containing compounds reported for the oxidation of *o*-phenylenediamine using hydrogen peroxide [12,13] and H<sub>2</sub>SO<sub>4</sub> [2] as oxidant. However non heme type iron(III) complexes that carry out the oxidation of *o*-phenylenediamine are scarce. In view of this we have synthesized new Fe(III) bis-benzimidazolyl diamide complexes and utilized them for the oxidation of *o*-phenylenediamine, in the presence of hydrogen peroxide. The effect of concentration of substrate, catalyst and anion has been studied with a view to gain insight into the mechanism of oxidation reaction.

## 2. Experimental

### 2.1. Analysis and physical measurements

Carbon, hydrogen, nitrogen and sulfur were estimated by using the Elemental Analyzer VARIO EL III at USIC, University of Delhi, Delhi. IR spectra were recorded in the solid state as KBr pellets on a Perkin-Elmer FTIR-2000 spectrometer. Electronic spectra were recorded in HPLC grade DMF on a Shimadzu 1601 spectrophotometer in the region of 200–1100 nm. <sup>1</sup>H NMR and <sup>13</sup>C spectra of ligand were recorded in *d*<sub>6</sub>-DMSO on a 400 MHz JEOL instrument at the Department of Chemistry, University of Delhi, Delhi. ESI mass spectra were recorded on a Agilent 6310 Ion Trap mass spectrometer in MeOH at INMAS, Defence Research and Development Organization, Delhi. Cyclic voltammetric studies were carried out on a BAS CV 50 W electrochemical analysis system in dimethyl sulfoxide (DMSO) at the Department of Chemistry, University of Delhi, Delhi. Mössbauer spectra of Fe(III) complexes were obtained using a <sup>57</sup>Co in Rh source, mounted on a constant acceleration

spectrometer WISSEL MB-550 at the GND University, Amritsar, Punjab. The velocity scale was calibrated using a foil of natural  $\alpha$ -Fe spectrum.

### 2.2. Materials

All the Solvents used were of HPLC grade. 2,5-Thiophenedicarboxylic acid was obtained from Aldrich. *o*-phenylenediamine was obtained from Merck. All chemicals were obtained from commercial sources and were used as received.

#### 2.2.1. Synthesis of *N*<sup>2</sup>, *N*<sup>5</sup>-bis((1*H*-benzo [*d*]imidazol-2-yl) methyl) thiophene-2,5-dicarboxamide (L)

The ligand was prepared following the procedure reported by Mathur et al. [14] and Vagg et al. [15]. Glycine benzimidazole dihydrochloride was prepared following the procedure reported by Cescon and Day [16] (see Scheme 1).

A solution of glycine benzimidazole dihydrochloride (5.0 g, 22.7 mmol) and 2,5-thiophenedicarboxylic acid (1.95 g, 11.4 mmol) in 20 ml pyridine was stirred for 5 min till a white precipitate was obtained. Then, triphenyl phosphite (TPP) (6.38 ml, 22.7 mmol) was added to the reaction mixture at a temperature of 50 °C and the temperature was slowly raised to 80–85 °C. Within half an hour, the precipitate redissolved and the clear solution was stirred for 30 h. The resulting orange brown solution was allowed to cool and washed with saturated NaHCO<sub>3</sub> solution in a separating funnel, till no effervescence could be seen. Then, it was washed with water 2–3 times. Upon further washing with acetone, a white solid precipitated. This was dried and washed with boiling methanol. This recrystallized white product was filtered, washed with cold water, dried in air and was analyzed for the composition C<sub>22</sub>H<sub>18</sub>N<sub>6</sub>O<sub>2</sub>S·2H<sub>2</sub>O.

Yield: 72%, M.P.:284–285 °C.

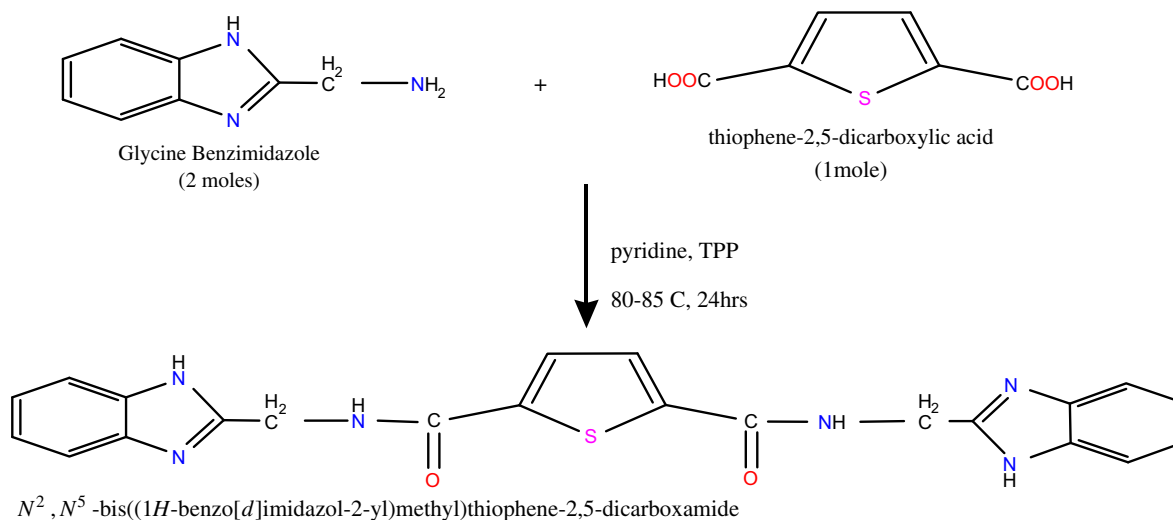
Anal. Found (Calc.) (%): C = 56.3(56.6), H = 5.3(4.7), N = 17.6(18.0), S = 7.3(6.8).

$\lambda_{\max}$  (nm), [log  $\epsilon$ ]: 284 [4.87], 277 [4.85].

### 2.3. Preparation of complexes

#### 2.3.1. Synthesis of complex [FeLCl<sub>2</sub>·2Cl]

To the ligand L (100 mg, 0.232 mmol) dissolved in DMF was added a methanolic solution (5 ml) of anhydrous FeCl<sub>3</sub> (37.7 mg, 0.232 mmol). The reaction mixture was stirred for 4 h at room temperature (30 °C) and then concentrated on a rotatory evapora-



Scheme 1. Synthesis of ligand.

tor. A light brown colored product was obtained by adding cold  $\text{CH}_3\text{CN}$  and it was filtered and washed with  $\text{MeOH}/\text{MeCN}$  (1:5).

The product analyzed for the composition  $\text{C}_{22}\text{H}_{18}\text{N}_6\text{O}_2\text{SFeCl}_3 \cdot 2\text{H}_2\text{O}$ , yield = 65%.

Anal. Found (Calc.) (%): C = 41.6(40.8), H = 4.1(3.8), N = 13.1(12.9), S = 5.1(4.9).

$\lambda_{\text{max}}$  (nm) [log  $\epsilon$ ] = 284 [4.55], 277 [4.53], 360 [3.21].

$m/z$  = 132, 300, 431, 462.

### 2.3.2. Synthesis of complex [FeLNO-3-2]-NO-3-

The nitrate complex was prepared by a similar procedure as above except that  $\text{Fe}(\text{NO}_3)_3 \cdot 9\text{H}_2\text{O}$  was used instead of  $\text{FeCl}_3$ . The product analyzed for the composition  $\text{C}_{22}\text{H}_{18}\text{N}_9\text{O}_{11}\text{SFe} \cdot \text{H}_2\text{O}$ , yield = 80%.

Anal. Found (Calc.) (%): C = 38.4(38.2), H = 3.0(2.8), N = 17.9(18.2), S = 4.6(4.6).

$\lambda_{\text{max}}$  (nm) [log  $\epsilon$ ] = 284 [3.54], 277 [3.52].

$m/z$  = 132, 300, 431, 542.

## 3. Result and discussion

### 3.1. Electronic spectroscopy

The UV Spectral data for the ligand and the complexes were taken in DMF. The ligand and complexes show bands in the region 281–274 nm. These bands are characteristics of the benzimidazole group and arise from the  $\pi \rightarrow \pi^*$  transitions [17]. A charge transfer band at 360 nm and at 354 nm is observed for the  $\text{Cl}^-$  and  $\text{NO}_3^-$  bound complexes and is assigned to the charge transfer  $\text{X}^- \rightarrow \text{Fe}$  [18].

### 3.2. IR spectral properties

The ligand and its iron(III) complexes have characteristic IR bands in the range  $1630\text{--}1675\text{ cm}^{-1}$ ,  $1545\text{--}1550\text{ cm}^{-1}$ ,  $1425\text{--}1445\text{ cm}^{-1}$ . These are assigned to amide I ( $\nu_{\text{C}=\text{O}}$  stretching) [19], amide II ( $\nu_{\text{C}-\text{N}}$  stretching) [20] and benzimidazole ring ( $\nu_{\text{C}-\text{N}=\text{C}}$

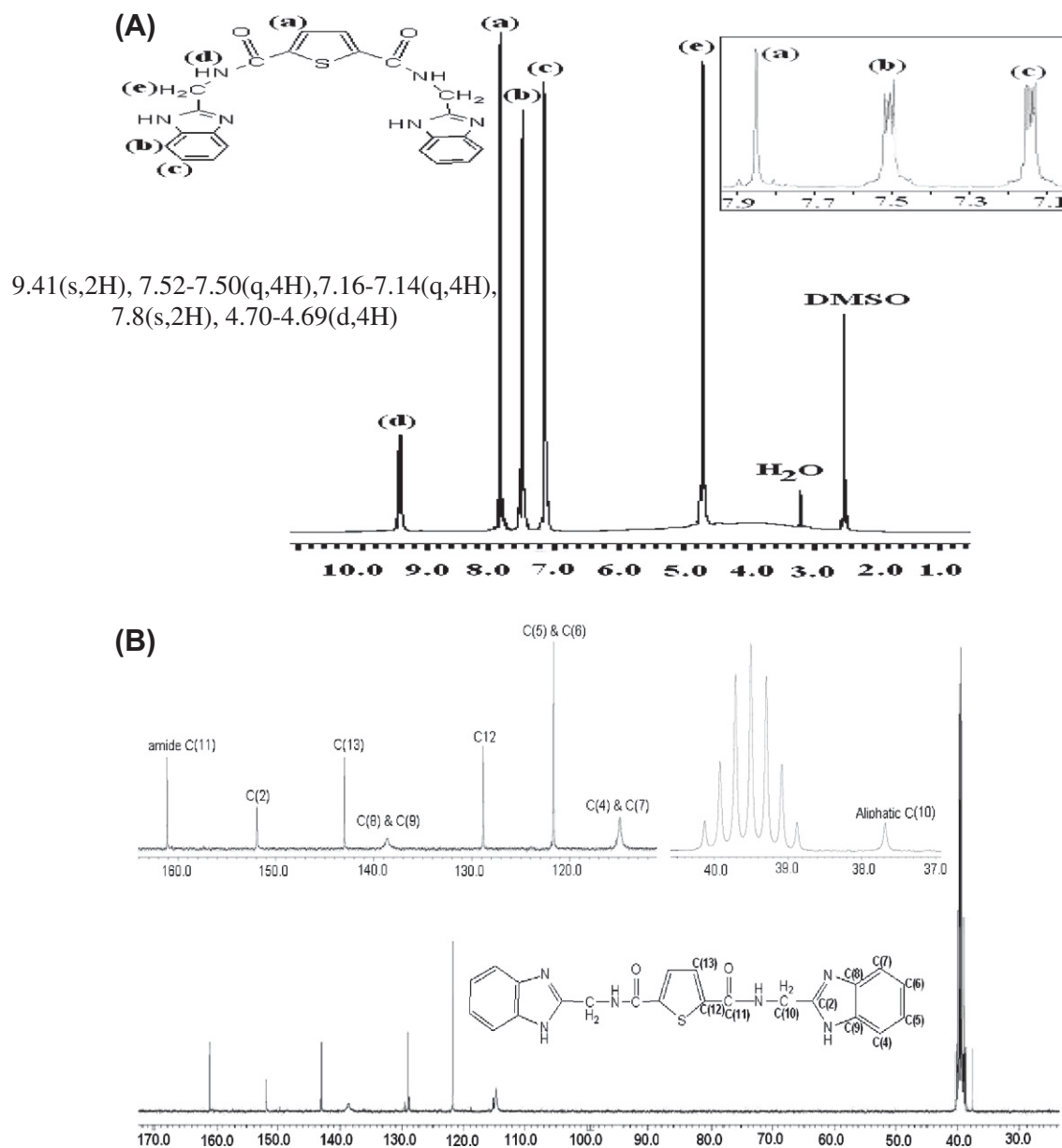


Fig. 1. (a)  $^1\text{H}$  NMR of the ligand L (b)  $^{13}\text{C}$  NMR of the ligand L.

stretching) [21]. The benzene ring gave a peak in the range of 735–745  $\text{cm}^{-1}$ . A very strong peak for the nitrate ion is observed at 1384  $\text{cm}^{-1}$  in the nitrate complex and is assigned to  $\nu_{\text{N-O}}$  stretching frequency [25a]. IR band appears at 1420, 1305 and 1008  $\text{cm}^{-1}$ . The separation of two highest bands is less (approx 100  $\text{cm}^{-1}$ ), this is indicative of a monodentate nitrate anion. [25b]. A broad band in the region 3300–3500  $\text{cm}^{-1}$  in the ligand and complexes assigned to O–H stretching. Shifts in the amide band I, due to C=O group and in amide II band due to C–N group, in the amide is indicative of the coordination of the ligand through the carbonyl oxygen in the complexes. benzimidazole N–H and amide N–H indicates the involvement of these groups either with the solvent or with the exogenous anion ligand [14,18]. IR shift reported in the text are similar to those of copper(II) complexes reported earlier by us on similar bis-benzimidazole diamide complexes. Several of our structural work on Cu(II) complexes with similar bis-benzimidazole ligands confirm the coordination of amide C=O and benzimidazole imine N, rather than amide NH; the shift in the IR region for the present complexes are similar to that found for copper(II) complexes reported [21–24].

### 3.3. $^1\text{H}$ NMR spectroscopy

$^1\text{H}$  NMR of the ligand shows signals for aliphatic and aromatic protons (Fig. 1a). A singlet is observed 9.41 ppm corresponding to N–H amide proton. Benzene ring protons are observed as multiplets in the range 7.5–7.1 ppm characteristics of AA' BB' pattern. The  $\text{CH}_2$  linked to benzimidazole group was observed at 4.70 ppm. The protons of thiophene ring are observed at 7.8 ppm.

$^{13}\text{C}$  NMR of the ligand peak show largest downfield shift for the C of amide followed by C(2), C(13), C(8) and C(9), C(12), C(5) and C(6), C(4) and C(7) and C(10) attached to amide –NH (Table 1, Fig. 1b).

### 3.4. Cyclic voltammetry

The cyclic voltammograms of complexes were recorded in DMSO solution with 0.1 M Tetrabutylammonium Perchlorate (TBAP) as a supporting electrolyte. A three-electrode configuration composed of Pt-disk working electrode, a Pt wire counter electrode, and an Ag/AgNO<sub>3</sub> reference electrode was used for measurements. The reversible one electron  $\text{Fc}^+/\text{Fc}$  (ferrocenium/ferrocene) couple has an  $E_{1/2}$  of +75 mV vs. Ag/AgNO<sub>3</sub>. The cyclic voltammograms display a quasi-reversible oxidation waves due to Fe(III)/Fe(II) couple (Fig. 2a and b, Supplementary material). The  $E_{1/2}$  of  $[\text{Fe}(\text{L})\text{Cl}_2]\cdot\text{Cl}$  and  $[\text{Fe}(\text{L})(\text{NO}_3)_2]\cdot\text{NO}_3$  complexes are found to be –267 mV and –144 mV, respectively. The value of  $E_{1/2}$  is more cathodic for  $[\text{Fe}(\text{L})\text{Cl}_2]\cdot\text{Cl}$  than  $[\text{Fe}(\text{L})(\text{NO}_3)_2]\cdot\text{NO}_3$  and confirms retention of anions in the coordination sphere of Fe(III). This also indicates that chloride anion stabilizes the iron(III) state in comparison to nitrate anion [26a].

### 3.5. Conductivity measurements

The molar conductivity values are measured in DMF. The values are found to be 48.2  $\text{S cm}^2 \text{mol}^{-1}$  and 97.5  $\text{S cm}^2 \text{mol}^{-1}$  for  $[\text{Fe}(\text{L})\text{Cl}_2]\cdot\text{Cl}$  and  $[\text{Fe}(\text{L})(\text{NO}_3)_2]\cdot\text{NO}_3$ , respectively. This indicates that at least one anion (chloride/nitrate) is dissociated in solution [26b].

### 3.6. EPR spectroscopy

The X-band EPR spectra of the Fe(III) complexes were recorded at liquid nitrogen temperature in DMSO (Fig. 3a and b, Supplementary material). The  $[\text{Fe}(\text{L})\text{Cl}_2]\cdot\text{Cl}$  complex gives a strong signal at  $g \sim 4.3$ , with weaker signals at  $g \sim 5.4$ ,  $g \sim 6.9$ . This is characteristic

**Table 1**  
 $^{13}\text{C}$  Chemical shift values for the ligand (L).

Chemical shift values	Assignments
37.6	Aliphatic –CH <sub>2</sub>
114.8	C(4), C(7)
121.8	C(5), C(6)
128.8	C(12)
138.7	C(8), C(9)
143.0	C(13)
151.9	C(2)
161.1	Amide C

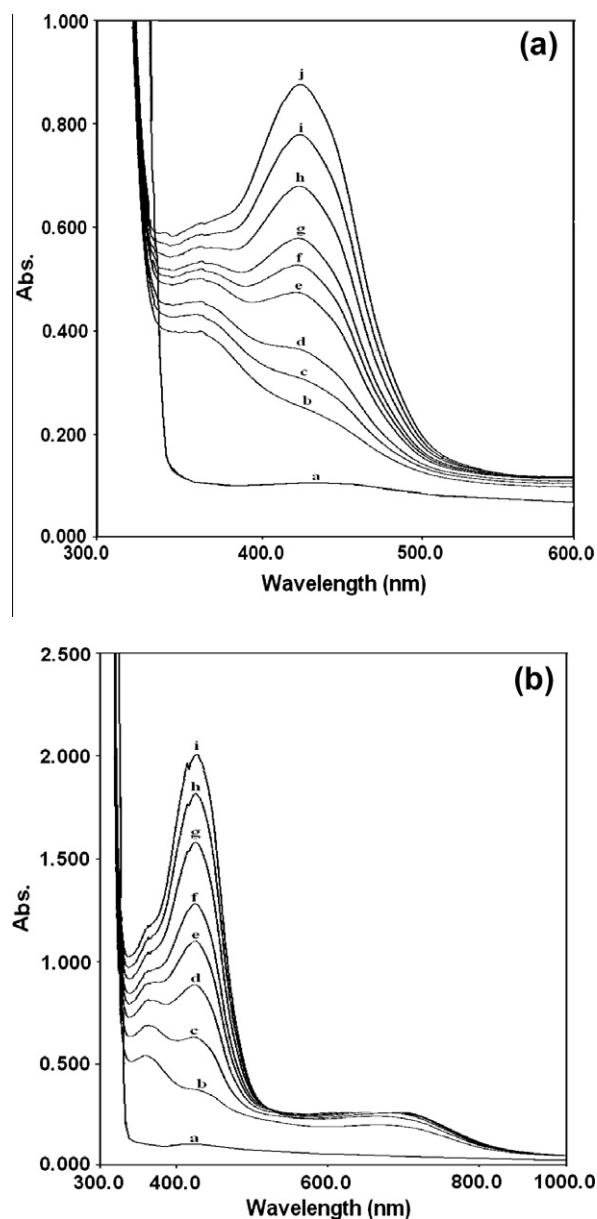


**Fig. 5.** (a) UV–VIS spectra of  $[\text{Fe}(\text{L})(\text{NO}_3)_2]\cdot\text{NO}_3 + o\text{-phenylenediamine}$  (1:40), in presence of  $\text{H}_2\text{O}_2$  (a)  $o\text{-pda}$  (6.0 mM) (b) at 1 min on adding complex (0.15 mM) (c) 5 min (d) 10 min (e) 20 min (f) 25 min (g) 30 min (h) 40 min (i) 50 min (j) 60 min, (b) UV–VIS spectra of  $[\text{Fe}(\text{L})\text{Cl}_2]\cdot\text{Cl} + o\text{-phenylenediamine}$  (1:40), in presence of  $\text{H}_2\text{O}_2$  (a)  $o\text{-phenylenediamine}$  (6.8 mM) (b) at 1 min on adding complex (0.17 mM) (c) 5 min (d) 10 min (e) 15 min (f) 20 min (g) 30 min (h) 40 min (i) 50 min.

of a rhombic complex undergoing an axial distortion, while  $[\text{Fe}(\text{L})(\text{NO}_3)_2]\cdot\text{NO}_3$  complex shows a strong signal at  $g = 2.4$ , and a weaker signal at  $g = 1.7$  representative of a six coordinated axially distorted complex [27,28a].

### 3.7. Mössbauer spectroscopy

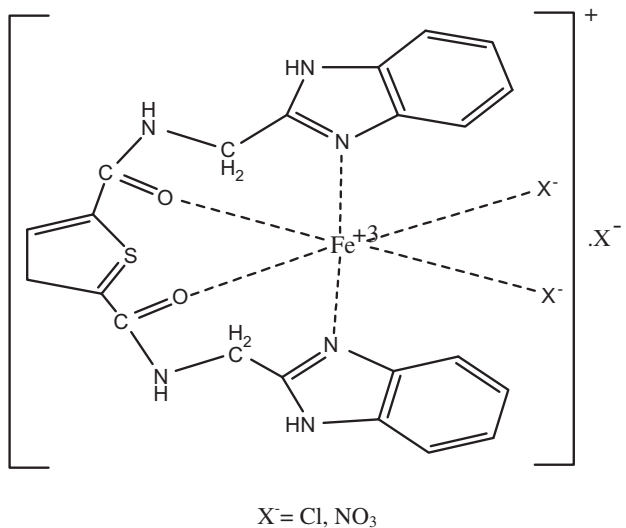
The  $^{57}\text{Fe}$  Mössbauer spectra of Fe(III) complexes were recorded at 298 K. (Fig. 4a and b, Supplementary material). Both spectra display a single quadrupole-split doublet. Quadrupole splitting for  $[\text{Fe}(\text{L})\text{Cl}_2]\cdot\text{Cl}$  is  $0.71\text{ mm s}^{-1}$  and isomeric shift is  $0.31\text{ mm s}^{-1}$ , while for complex  $[\text{Fe}(\text{L})(\text{NO}_3)_2]\cdot\text{NO}_3$  quadrupole splitting and isomeric shift are  $0.57\text{ mm s}^{-1}$  and  $1.70\text{ mm s}^{-1}$ . These parameters indicate a non symmetrical charge distribution around the Fe(III) center and the existence of distorted octahedral high spin Fe(III) ions [26a,28b–f].

### 3.8. Mass spectroscopy

ESI Mass spectra have been taken in MeOH. Base peak was found at 431 and is assigned to the intact ligand  $\text{C}_{22}\text{H}_{18}\text{N}_6\text{O}_2\text{S} + \text{H}^+$ . Fragment at 132 corresponds to benzimidazolyl ring:  $\text{C}_8\text{H}_7\text{N}_2 + \text{H}^+$ , while fragment at 300 corresponds to:  $\text{C}_{22}\text{H}_{18}\text{N}_6\text{O}_2\text{S}-132$ . These are mass peaks related to the ligand. Fragment related to the complex  $[\text{Fe}(\text{L})\text{Cl}_2]\cdot\text{Cl}$  is assigned at 462 and corresponds to  $[\text{C}_{22}\text{H}_{18}\text{N}_6\text{O}_2\text{S}-\text{FeCl}_3-132]$ . Fragment related to the complex  $[\text{Fe}(\text{L})(\text{NO}_3)_2]\cdot\text{NO}_3$  is assigned at 542 and correspond to  $[\text{C}_{22}\text{H}_{18}\text{N}_9\text{O}_{11}\text{SFe}-132]$ .

#### Tentative structure of complexes

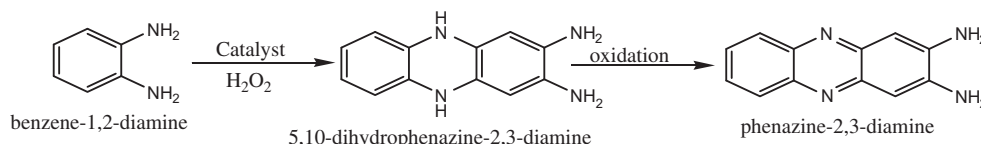
On the basis of EPR, Mass, Conductivity measurements and Mössbauer Spectra following tentative structure have been proposed:



## 4. Reactivity of $[\text{Fe}(\text{L})\text{Cl}_2]\cdot\text{Cl}$ and $[\text{Fe}(\text{L})(\text{NO}_3)_2]\cdot\text{NO}_3$

### 4.1. Oxidation of *o*-phenylenediamine

*o*-Phenylenediamine oxidizes to form 2,3-diaminophenazine in the presence of  $\text{H}_2\text{O}_2$  (Scheme 2) [3,6]. Both the  $[\text{Fe}(\text{L})\text{X}_2]\cdot\text{X}$  complexes were utilized as catalyst to oxidize *o*-phenylenediamine in



Scheme 2. Reaction for the oxidation of *o*-phenylenediamine.

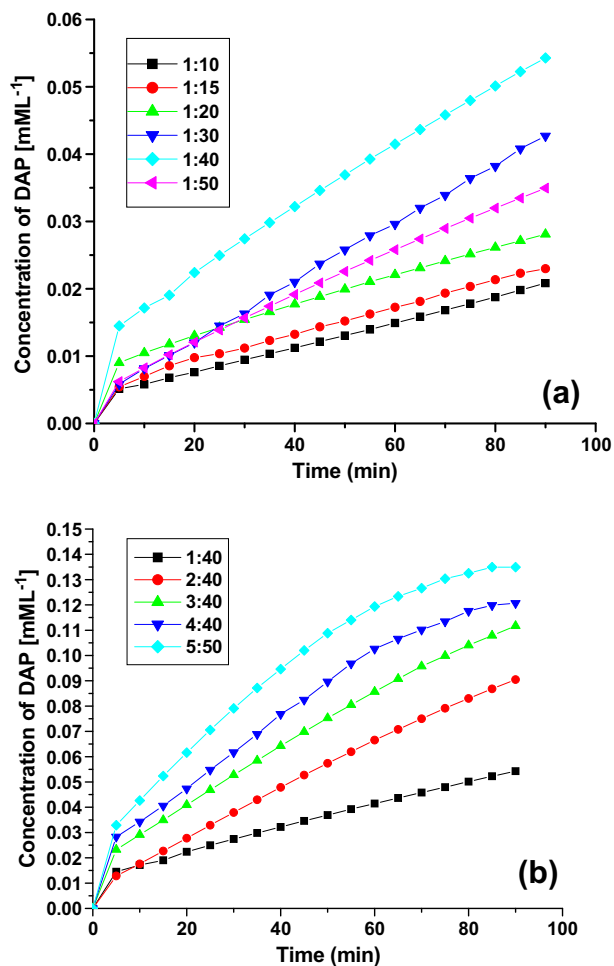


Fig. 6. (a) Effect of concentration of substrate on rate of reaction for  $[\text{Fe}(\text{L})(\text{NO}_3)_2]\cdot\text{NO}_3$ -catalyzed oxidation of *o*-phenylenediamine, (b) effect of concentration of catalyst on rate of reaction for  $[\text{Fe}(\text{L})(\text{NO}_3)_2]\cdot\text{NO}_3$ -catalyzed oxidation of *o*-phenylenediamine.

the presence of  $\text{H}_2\text{O}_2$ . Spectrophotometry was used to study the kinetics of the oxidation reaction, for which the absorbance of the reaction product 2,3-diaminophenazine at 425 nm was recorded with the time. The reaction is as follows.

### 4.2. General procedure

A 0.75 mM (5 ml) methanolic solution of iron(III) complex was added to a methanolic solution of *o*-phenylenediamine, 29.7 mM (5 ml) and  $\text{H}_2\text{O}_2$ , 5.8 mM (0.02 ml). One ml of this reaction mixture is diluted to make 5 ml and absorption spectra were recorded with time in the range 300–1100 nm at room temperature, for a period of 60 min. A new band at 425–430 nm starts to increase which confirms the formation of 2,3-diaminophenazine. Simultaneously a new band at 725 nm also starts to form. A blank experiment (oxidation of OPD with  $\text{H}_2\text{O}_2$  without the Fe(III) complex) was also carried out. No oxidation of *o*-phenylenediamine was found during a 60 min period.

To study the effect of anions like acetate, azide and citrate, the sodium salts of these anions were added in comparable ratio to the catalyst used, and effect of this on the rate of reaction, was studied.

#### 4.3. Kinetic studies

The kinetic studies on the oxidation of *o*-phenylenediamine were carried out by monitoring the increase in the characteristic 2,3-diaminophenazine absorption band at 425–430 nm as a function of time (Fig. 5a and b). The concentration of product formed was calculated using the extinction coefficient of 2,3-diaminophenazine,  $\epsilon = 2.1 \times 10^4 \text{ M}^{-1} \text{ cm}^{-1}$  [1]. To determine the dependence of the rates on the substrate concentration, solutions of the complex  $[\text{Fe}(\text{L})\text{X}_2]\cdot\text{X}$  were treated with increasing amounts of *o*-phenylenediamine. To determine the dependence of the rates on the catalyst concentration, solutions of the *o*-phenylenediamine were treated with increasing amounts of  $[\text{Fe}(\text{L})\text{X}_2]\cdot\text{X}$ , at least two sets of data were taken (Figs. 6a,b and 7a,b). The graphs between initial rates and concentration of *o*-phenylenediamine and Catalyst were plotted (Figs. 8a,b and 9a,b). The initial rates of reactions for the various sets are combined in Tables 2a, 2b and 3a, 3b). For the pseudo first order dependence vs. substrate behaviour it has been found that the kinetics follow a pseudo first order up to a ratio of catalyst:substrate (1:30) beyond which if the concentration of

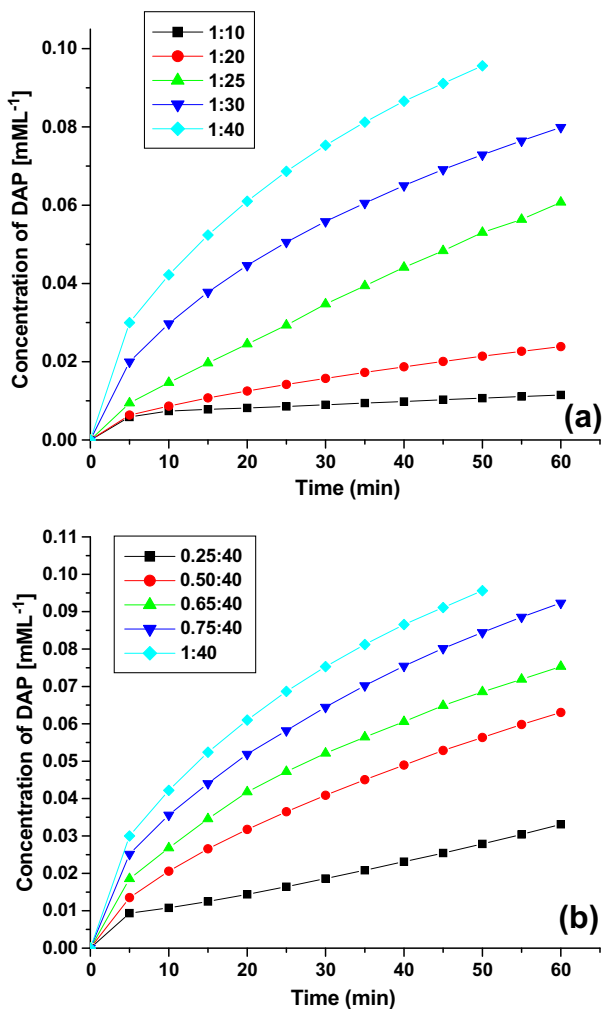


Fig. 7. (a) Effect of concentration of substrate on rate of reaction for  $[\text{Fe}(\text{L})\text{Cl}_2]\cdot\text{Cl}$ -catalyzed oxidation of *o*-phenylenediamine, (b) effect of concentration of catalyst on rate of reaction for  $[\text{Fe}(\text{L})\text{Cl}_2]\cdot\text{Cl}$ -catalyzed oxidation of *o*-phenylenediamine.

the substrate is increased a saturation is observed. Thus it appears that pseudo first order kinetics is followed only up to a catalyst:substrate ratio of (1:30).

The optimum rate of reaction is found when the ratio between catalysts and substrate is 1:40. The rate was  $14.1 \times 10^{-4} \text{ mM L}^{-1} \text{ min}^{-1}$  and  $66.7 \times 10^{-4} \text{ mM L}^{-1} \text{ min}^{-1}$  for the catalyst  $[\text{Fe}(\text{L})(\text{NO}_3)_2]\cdot\text{NO}_3$  and  $[\text{Fe}(\text{L})\text{Cl}_2]\cdot\text{Cl}$ , respectively. The reaction is faster in the presence of complex  $[\text{Fe}(\text{L})\text{Cl}_2]\cdot\text{Cl}$ . The initial rate of reaction is found to be dependent on both the concentration of *o*-phenylenediamine as well as the iron(III) complex, while keeping the concentration of hydrogen peroxide constant at an optimum molarity. Thus the oxidation reaction is a second order reaction following the rate equation:

$$\text{Rate} = k[\textit{o}\text{-phenylenediamine}][\text{Iron(III)complex}]$$

#### 4.4. Formation of intermediate

When the complex  $[\text{Fe}(\text{L})\text{Cl}_2]\cdot\text{Cl}$  is mixed with *o*-phenylenediamine (1.12 mM and 45 mM), weak bands are generated at around 430 nm, 450 nm and 480 nm (Fig. 10). The presence of a weak band at 430 nm suggests that small amount of 2,3-diaminophenazine is formed even in the absence of the oxidant  $\text{H}_2\text{O}_2$ . The presence of

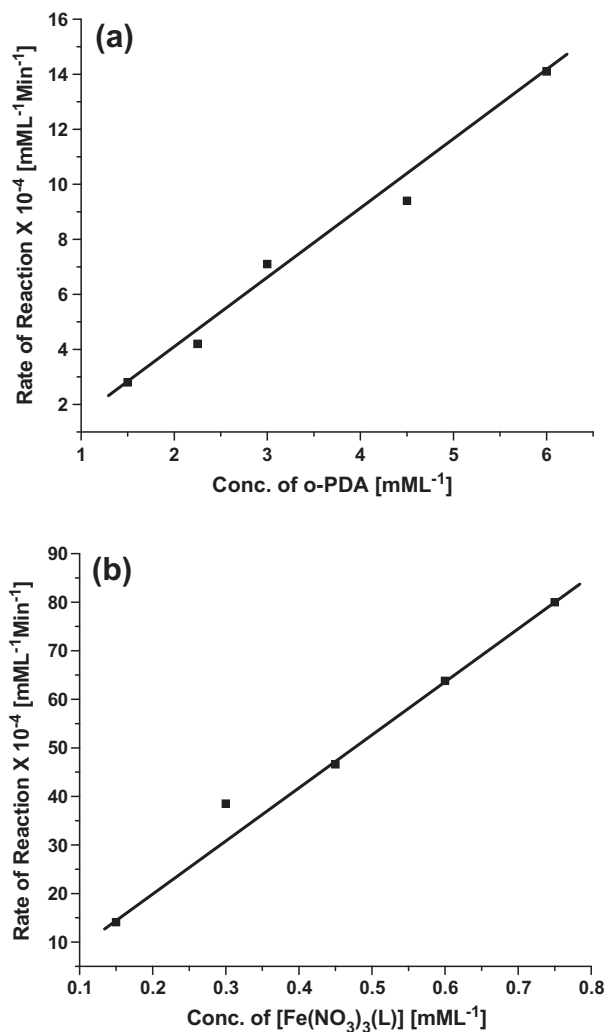
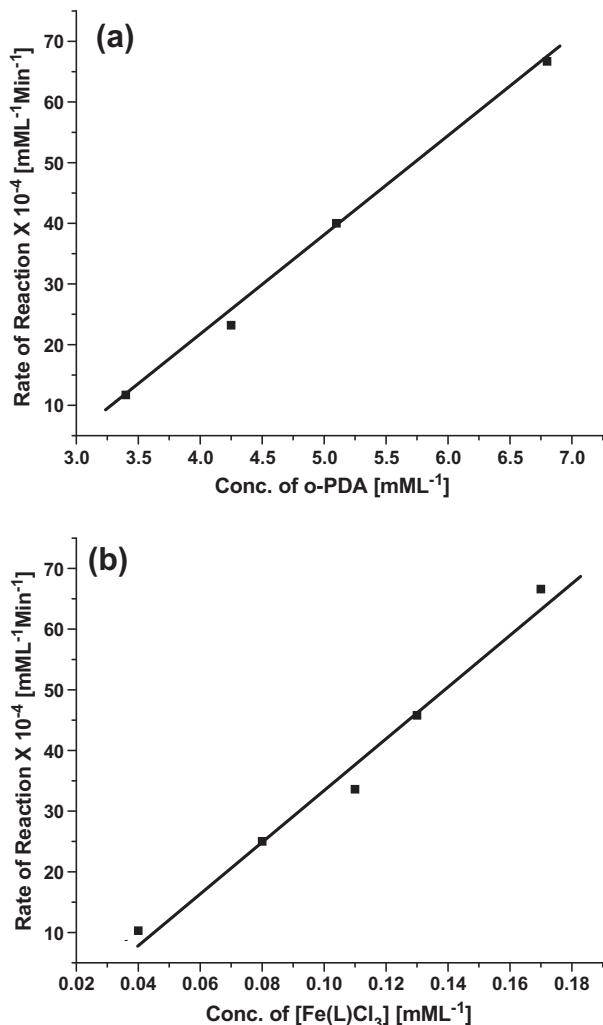


Fig. 8. (a) Concentration of *o*-phenylenediamine vs. initial rate of reaction for  $[\text{Fe}(\text{L})(\text{NO}_3)_2]\cdot\text{NO}_3$ -catalyzed oxidation of *o*-phenylenediamine, (b) concentration of catalyst vs. initial rate of reaction for  $[\text{Fe}(\text{L})(\text{NO}_3)_2]\cdot\text{NO}_3$ -catalyzed oxidation of *o*-phenylenediamine.



**Fig. 9.** (a) Concentration of *o*-phenylenediamine vs. initial rate of reaction for [Fe(L)Cl $_2$ ].Cl-catalyzed oxidation of *o*-phenylenediamine, (b) concentration of catalyst vs. initial rate of reaction for [Fe(L)Cl $_2$ ].Cl-catalyzed oxidation of *o*-phenylenediamine.

**Table 2a**

Kinetic data for the [Fe(L)(NO $_3$ ) $_2$ ].NO $_3$ -catalyzed oxidation of *o*-phenylenediamine (variation in concentration of OPDA).

S. No.	Concentration of [Fe(L)(NO $_3$ ) $_2$ ].NO $_3$ (mM)	Concentration of <i>o</i> -phenylenediamine (mM)	Initial rate of reaction $\times 10^{-4}$ (mM L $^{-1}$ min $^{-1}$ )	Ratio of cata.:sub
1	0.15	1.5	2.8	1:10
2	0.15	2.25	4.2	1:15
3	0.15	3.0	7.1	1:20
4	0.15	4.5	9.4	1:30
5	0.15	6.0	14.1	1:40
6	0.15	7.5	12.7	1:50

**Table 2b**

Kinetic data for the [Fe(L)(NO $_3$ ) $_2$ ].NO $_3$ -catalyzed oxidation of *o*-phenylenediamine (variation in concentration of catalyst).

S. No.	Concentration of [Fe(L)(NO $_3$ ) $_2$ ].NO $_3$ (mM)	Concentration of <i>o</i> -phenylenediamine (mM)	Initial rate of reaction $\times 10^{-4}$ (mM L $^{-1}$ min $^{-1}$ )	Ratio of cata.:sub
1	0.15	6.0	14.1	1:40
2	0.30	6.0	38.4	2:40
3	0.45	6.0	46.6	3:40
4	0.60	6.0	63.8	4:40
5	0.75	6.0	80.0	5:40

**Table 3a**

Kinetic data for the [Fe(L)Cl $_2$ ].Cl-catalyzed oxidation of *o*-phenylenediamine (variation in concentration of OPDA).

S. No.	Concentration of [Fe(L)Cl $_2$ ].Cl (mM)	Concentration of <i>o</i> -phenylenediamine (mM)	Initial rate of reaction $\times 10^{-4}$ (mM L $^{-1}$ min $^{-1}$ )	Ratio of cata.:sub
1	0.17	1.7	7.8	1:10
2	0.17	3.4	11.7	1:20
3	0.17	4.25	23.2	1:25
4	0.17	5.1	40.0	1:30
5	0.17	6.8	66.7	1:40

**Table 3b**

Kinetic data for the [Fe(L)Cl $_2$ ].Cl-catalyzed oxidation of *o*-phenylenediamine (variation in concentration of catalyst).

S. No.	Concentration of [Fe(L)Cl $_2$ ].Cl (mM)	Concentration of <i>o</i> -phenylenediamine (mM)	Initial rate of reaction $\times 10^{-4}$ (mM L $^{-1}$ min $^{-1}$ )	Ratio of cata.:sub
1	0.04	6.8	10.3	0.25:40
2	0.08	6.8	25.0	0.50:40
3	0.11	6.8	33.6	0.65:40
4	0.13	6.8	45.8	0.75:40
5	0.17	6.8	66.7	1:40

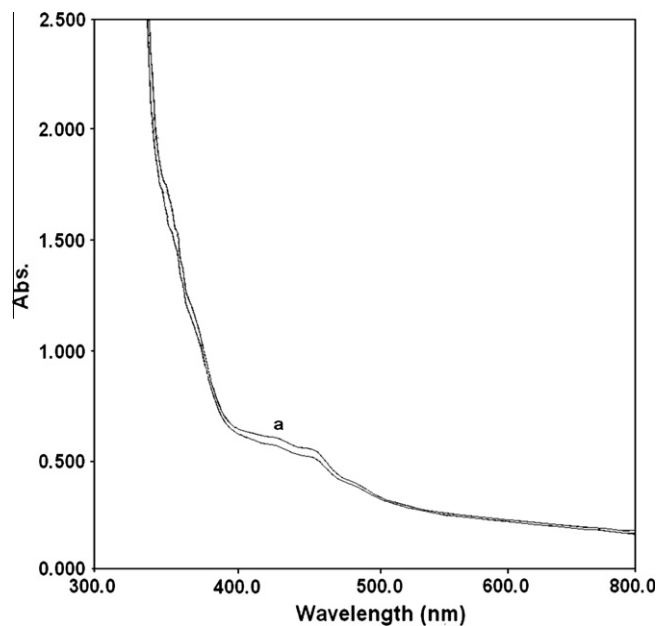


**Fig. 10.** UV-VIS spectra of [Fe(L)Cl $_2$ ].Cl + *o*-phenylenediamine (1:40), in absence of H $_2$ O $_2$  (a) 30 min.

**Table 4a**

Kinetic data for the [Fe(L)(NO $_3$ ) $_2$ ].NO $_3$ -catalyzed oxidation of *o*-phenylenediamine in the presence of different anions.

S. No.	Concentration of anion (mM)	Type of anion	Initial rate of reaction $\times 10^{-4}$ (mM L $^{-1}$ min $^{-1}$ )	Ratio b/w cata. vs. subs. and anion
1	–	Without any externally added anion	14.1	1:40
2	0.15	Acetate ion	8.6	1:40:1
3	0.15	Azide ion	4.3	1:40:1
4	0.15	Citrate ion	1.0	1:40:1

**Table 4b**

Kinetic data for the  $[\text{Fe}(\text{L})\text{Cl}_2]\text{-Cl}$ -catalyzed oxidation of *o*-phenylenediamine in the presence of different anions.

S. No.	Concentration of anion (mM)	Type of anion	Initial rate of reaction $\times 10^{-4}$ ( $\text{mM L}^{-1} \text{min}^{-1}$ )	Ratio b/w cata. vs. subs. and anion
1	–	Without any externally added anion	66.7	1:40
2	0.17	Acetate ion	33.3	1:40:1
3	0.17	Azide ion	18.2	1:40:1
4	0.17	Citrate ion	9.8	1:40:1

**Table 5**

kinetic data for the  $[\text{Fe}(\text{L})(\text{NO}_3)_2]\text{-NO}_3$ -catalyzed oxidation of *o*-phenylenediamine (role of  $\text{H}_2\text{O}_2$ ).

S. No.	Concentration of $[\text{Fe}(\text{L})(\text{NO}_3)_2]\text{-NO}_3$ (mM)	Concentration of OPDA (mM)	Concentration of $\text{H}_2\text{O}_2$ (mM)	Initial rate of reaction $\times 10^{-4}$ ( $\text{mM L}^{-1} \text{min}^{-1}$ )
1	0.15	1.5	2.9	18.8
2	0.15	1.5	5.8	32.2
3	0.15	1.5	11.6	34.2

different from the species generated due to a weak interaction of *o*-phenylenediamine and iron(III) complex.

#### 4.5. Effect of presence of other anions

An experiment was carried out to check the effect of anions like acetate, azide or citrate (added as sodium salts) on the rate of formation of diaminophenazine (DAP). For this experiment the concentration of *o*-phenylenediamine and  $[\text{Fe}(\text{L})(\text{NO}_3)_2]\text{-NO}_3$  was kept at 6.0 mM, 0.15 mM and 6.8 mM, 0.17 mM in case of  $[\text{Fe}(\text{L})\text{Cl}_2]\text{-Cl}$  as the catalyst. Different anions were added in such amount so as to keep the ratio of anion to catalyst as 1:1. Addition of different anions to the reaction mixture of *o*-phenylenediamine,  $\text{H}_2\text{O}_2$  and  $[\text{Fe}(\text{L})(\text{NO}_3)_2]\text{-NO}_3$  or  $[\text{Fe}(\text{L})\text{Cl}_2]\text{-Cl}$  results in the inhibition

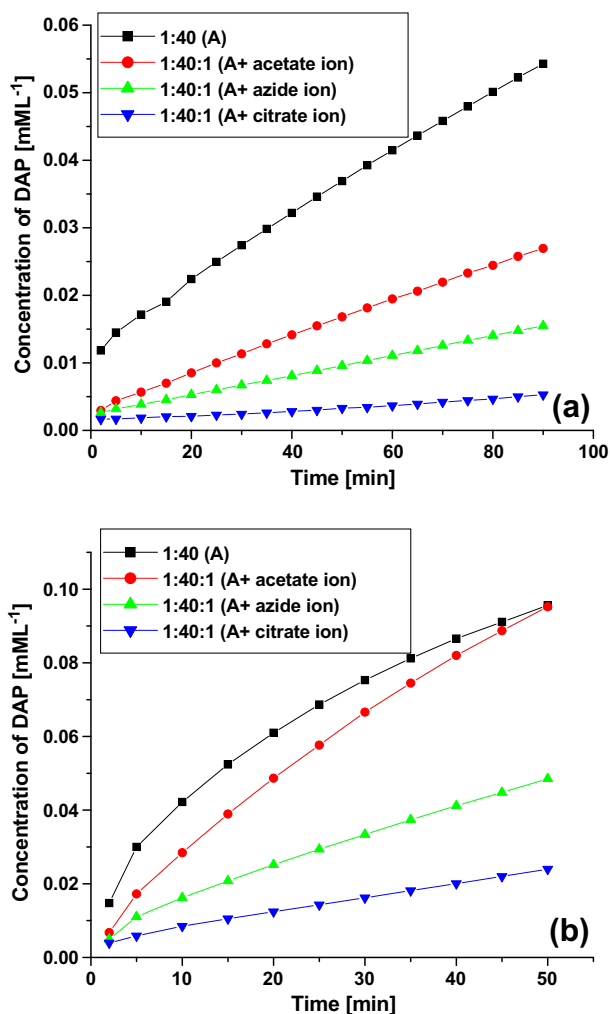


**Fig. 11.** (a) Effect of presence of external anions (acetate, azide, citrate) on rate of reaction for  $[\text{Fe}(\text{L})(\text{NO}_3)_2]\text{-NO}_3$ -catalyzed oxidation of *o*-phenylenediamine, (b) effect of presence of external anions (acetate, azide, citrate) on rate of reaction for  $[\text{Fe}(\text{L})\text{Cl}_2]\text{-Cl}$ -catalyzed oxidation of *o*-phenylenediamine.

other new bands at 450, 480 nm are indicative of an interaction between *o*-phenylenediamine and the iron(III) complex. However on the addition of  $\text{H}_2\text{O}_2$  to the solution containing the iron(III) complex and *o*-phenylenediamine, there is a rapid increase in the band at 430 nm and simultaneously a new band generates at  $\sim 725$  nm. The band at 725 nm has been attributed to the formation of an intermediate related to *o*-phenylenediamine, which forms during the oxidation reaction [29]. This band grows slowly, along with the band at 430 nm. Thus the intermediate species at 725 nm, is

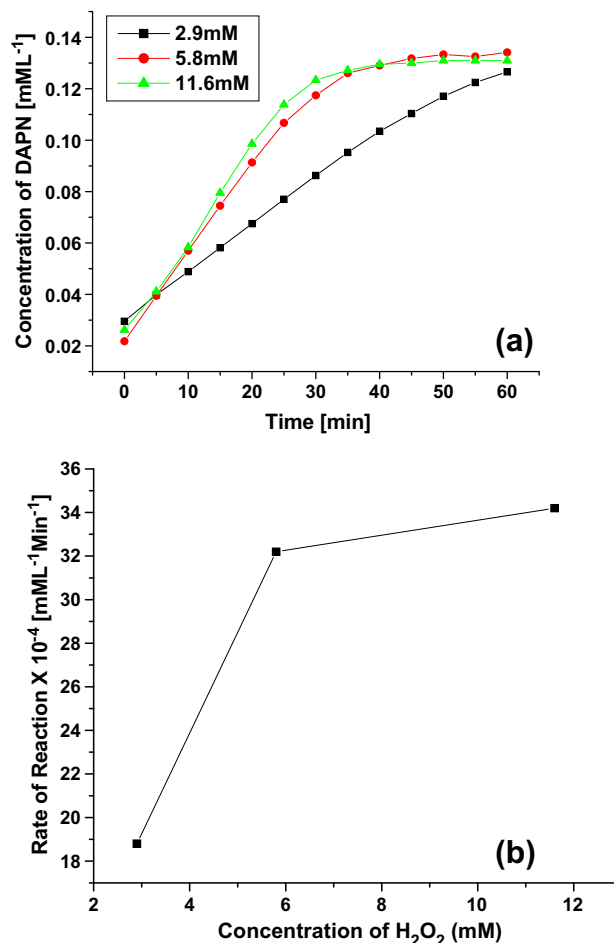


**Fig. 12.** (a) Effect of Concentration of  $\text{H}_2\text{O}_2$  on rate of reaction for  $[\text{Fe}(\text{L})(\text{NO}_3)_2]\text{-NO}_3$ -catalyzed oxidation of *o*-phenylenediamine, (b) concentration of  $\text{H}_2\text{O}_2$  vs. initial rate of reaction for  $[\text{Fe}(\text{L})(\text{NO}_3)_2]\text{-NO}_3$ -catalyzed oxidation of *o*-phenylenediamine.

of the formation of 2,3-diaminophenazine. The initial rate of reaction decreases and the kinetic data is shown in Tables 4a and 4b Fig. 11a and b. The order of quenching of the initial rate of reaction is: acetate ion < azide ion < citrate ion. This order is same for both of the catalysts. A experiment was conducted to ascertain whether addition of different anions to the catalyst [Fe(L)Cl<sub>3</sub>] or [Fe(L)(-NO<sub>3</sub>)<sub>3</sub>] in the absence of the substrate show any changes in the UV–VIS spectra. It is found that addition of the anion acetate, azide and citrate cause a shift in the UV band by 5–7 nm, suggesting that binding of these anions occurs at the iron(III) centre. In the case of the azide anion, addition causes a new shoulder to appear at 425 nm confirming the above.

#### 4.6. Role of H<sub>2</sub>O<sub>2</sub>

The effect of varying the concentration of H<sub>2</sub>O<sub>2</sub> on the initial rate of reaction was also studied. For this the concentration of catalyst (0.15 mM) and *o*-phenylenediamine (1.5 mM) was kept constant and concentration of H<sub>2</sub>O<sub>2</sub> was varied (Table 5). It is clear from the Fig. 12a and b that as the concentration of H<sub>2</sub>O<sub>2</sub> increases (2.9 mM (0.01 ml), 5.8 mM (0.02 ml) and 11.6 mM (0.04 ml)) rate of reaction increases, to an optimum value and then stabilizes. As the volume of added aqueous H<sub>2</sub>O<sub>2</sub> was very small hence it is assumed that any displacement of anions by H<sub>2</sub>O molecules is insignificant. The concentration of H<sub>2</sub>O<sub>2</sub> is not included in the rate equation because upon increasing the H<sub>2</sub>O<sub>2</sub> molarity a optimum rate is observed for a molarity up to 5.8 mM. The optimum molarity of H<sub>2</sub>O<sub>2</sub> has been fixed for each set of variation in catalyst/substrate concentration. An experiment was conducted to ascertain whether there may not be a direct interaction of the complex with hydrogen peroxide (catalase activity). Thus the iron complex was treated with H<sub>2</sub>O<sub>2</sub> and a UV visible recorded. It was found that no change takes place in either the charge transfer band nor the UV bands of the ligands implying no change in the oxidation state of the Iron centre in the complexes.

## 5. Conclusions

- Since the reduction potential of [Fe(L)Cl<sub>2</sub>].Cl complex is more cathodic than the [Fe(L)(NO<sub>3</sub>)<sub>2</sub>].NO<sub>3</sub> complex, it was expected that the latter should be a better oxidizing agent, leading to higher rates oxidation of *o*-phenylenediamine. However, it is found that the rates of reaction are faster with [Fe(L)Cl<sub>2</sub>].Cl than [Fe(L)(NO<sub>3</sub>)<sub>2</sub>].NO<sub>3</sub>.
- This suggests that the rate determining step is controlled by other factors than thermodynamic oxidation potentials of the complexes.
- Further we have looked at oxidation reaction in the presence of anions (acetate, azide, and citrate). These anions have larger binding constants to iron(III) than those reported for Cl<sup>-</sup> and NO<sub>3</sub><sup>-</sup>.
- The rates were found to decrease in the order acetate ion < azide ion < citrate ion.
- This suggests that one of the factor affecting the rate determining step is the binding of these anions at a vacant site on the Fe<sup>3+</sup> complexes, created by the loss of Cl<sup>-</sup>/NO<sub>3</sub><sup>-</sup>. The rate drops because the anions compete with the binding of *o*-phenylenediamine to the iron(III) center, and this is supported by UV visible experiments.
- As there is a substantial effect of anion on the rate of reaction. This implies a role for the Iron(III) centre in the oxidation of *o*-phenylenediamine. This oxidation could be achieved by an inner sphere electron transfer process between the iron(III) centre and the weakly bound *o*-phenylenediamine.

- In the reaction the H<sub>2</sub>O<sub>2</sub> is consumed so the rate of reaction is increased as the concentration of H<sub>2</sub>O<sub>2</sub> is increased, up to an optimum value.

## Acknowledgement

Financial support of the Council of Scientific and Industrial Research (01(2218)08/EMRII) and University of Delhi is gratefully acknowledged. The authors are grateful to Ravinder Kumar(UGC-JRF) for helping in preparing the revised manuscript.

## Appendix A. Supplementary data

Supplementary data associated with this article can be found, in the online version, at <http://dx.doi.org/10.1016/j.saa.2012.07.004>.

## References

- [1] V.M. Mekler, O.V. Belonogova, V.I. Nikulin, J. Photochem. Photobiol. A: Chem. 87 (1995) 243–247.
- [2] F.S. Damos, M.P.T. Sotomayor, L.T. Kubota, S.M.C.N. Tanaka, A.A. Tanaka, Analyst 128 (2003) 255–259.
- [3] P.J. Tarcha, V.P. Chu, D. Whittern, Anal. Biochem. 165 (1987) 230–233.
- [4] S. Kawakubo, Y. Hagihara, Y. Honda, M. Iwatsuki, Anal. Chim. Acta 388 (1999) 35–43.
- [5] C. Hemen, S.M.V. Leeuwen, H. Luftmann, U. Karst, Anal. Bioanal. Chem. 382 (2005) 234–238.
- [6] D.J. Li, X.W. Li, Y.X. Xie, X.Q. Cai, G.L. Zou, Biochemistry 70 (2005) 92–99.
- [7] K. Zhang, R. Cai, D. Chen, L. Mao, Anal. Chim. Acta 413 (2000) 109–113.
- [8] O. Altun, E. Dolen, M. Pekin, H.Y. Aboul-Enein, Instrum. Sci. Technol. 31 (2003) 15–21.
- [9] L.I. Simandi, T. Barna, Z. Szeverenyi, S. Nemeth, Pure Appl. Chem. 64 (1992) 1511–1518.
- [10] L.I. Simandi, T.M. Simandi, Z. May, G. Besenyei, Coord. Chem. Rev. 245 (2003) 85–93.
- [11] A.B. Zaki, M.Y. El-Seikh, J. Evans, S.A. El-Safty, Polyhedron 19 (2000) 1317–1328.
- [12] V.M. Mekler, S.M. Bystryak, J. Photochem. Photobiol. A: Chem. 65 (1992) 391–397.
- [13] E.Yu. Pisarevskaya, E.V. Ovsyannikova, L.P. Kazanskii, N.M. Alpatova, Russ. J. Electrochem. 40 (2010) 1042–1046.
- [14] (a) F. Afreen, A. Rheingold, P. Mathur, Inorg. Chim. Acta 358 (2005) 1125–1134;  
(b) M. Gupta, R.J. Butcher, P. Mathur, Inorg. Chem. 40 (2001) 878–885.
- [15] D.J. Barnes, R.L. Chapman, R.S. Vagg, E.C. Watton, J. Chem. Eng. Data 23 (1978) 349–350.
- [16] L.A. Cescon, A.R. Day, J. Org. Chem. 27 (1962) 581–586.
- [17] E. Monzani, L. Quintini, A. Perotti, L. Casella, M. Gullotti, L. Randaccio, S. Geremia, G. Nardin, P. Faleschini, G. Tabbi, Inorg. Chem. 37 (1998) 553–562.
- [18] S. Tehlan, M.S. Hundal, P. Mathur, Inorg. Chem. 43 (2004) 6589–6595.
- [19] S.C. Mohapatra, S. Tehlan, M.S. Hundal, P. Mathur, Inorg. Chim. Acta 361 (2008) 1897–1907.
- [20] R. Bakshi, P. Mathur, Inorg. Chim. Acta 363 (2010) 3477–3488.
- [21] P. Mathur, M. Crowder, G.C. Dismukes, J. Am. Chem. Soc. 109 (1987) 5227–5233.
- [22] G. Ahuja, P. Mathur, Inorg. Chem. Commun. 17 (2012) 42–48.
- [23] R. Bakshi, M. Rossi, F. Caruso, P. Mathur, Inorg. Chim. Acta 376 (2011) 175–188.
- [24] S.C. Mahapatra, P. Mathur, Spectrochim. Acta 78 (2011) 612–616.
- [25] (a) S. Menage, L. Que Jr, Inorg. Chem. 29 (1990) 4293–4297;  
(b) B.M. Gatehouse, S.E. Livigstone, R.S. Nyholm, J. Chem. Soc. (1957) 4222–4225.
- [26] (a) V. Arora, Rajesh, P. Mathur, Transition Met. Chem. 24 (1999) 92–94;  
(b) W.J. Geary, Coord. Chem. Rev. 7 (1971) 81–122.
- [27] D.C. Finnen, A.A. Pinkerton, W.R. Dunham, R.H. Sandr, M.O. Funk Jr., Inorg. Chem. 30 (1991) 3960–3963.
- [28] (a) G. Batra, P. Mathur, Polyhedron 12 (1993) 2635–2643;  
(b) X. Wang, S. Wang, L. Li, E.B. Sundberg, G.P. Gacho, Inorg. Chem. 42 (2003) 7799–7808;  
(c) E.W. Ainscough, A.M. Brodie, J.E. Plowman, V.L. Brown, A.W. Addison, A.R. Gainsford, Inorg. Chem. 19 (1980) 3655–3663;  
(d) W.H. Armstrong, A. Spool, G.C. Papaefthymiu, R.B. Frankel, S.J. Lippard, J. Am. Chem. Soc. 106 (1984) 3653–3667;  
(e) H.N. Pandey, P. Mathur, Transition Met. Chem. 20 (1995) 144–146;  
(f) H. Adam, N.A. Bailey, J.D. Crane, D.E. Fenton, J.-M. Latour, J.M. Williams, J. Chem. Soc. Dalton Trans. (1990) 1727–1735.
- [29] L. Hai-cheng, L. De-jia, H. Bo, J. De-long, Z. Guo-lin, Wuhan Univ. J. Nat. Sci. 7 (2002) 117–121.